ICSV14
Cairns • Australia
9-12 July, 2007

14th International Congress on Sound & Vibration

# A 3D NUMERICAL METHOD TO STUDY POROELASTIC LINERS WITH MEAN FLOW

Benoit Nennig, Mabrouk Ben Tahar, Emmanuel Perrey-Debain

Laboratoire Roberval FRE 2833, Département acoustique,
Université de Technologie de Compiègne,
BP 20529,60205 Compiègne cedex, France

benoit.nennig@utc.fr

**Abstract**

In this paper, we study the noise attenuation in poroelastic liners exposed to grazing flow. The acoustic propagation in the liner and in the aeroacoustic domain are respectively governed by Biot's model and Galbrun's equation. Here, the coupling between Galbrun's and Biot's equation is realized with a mixed pressure-displacement finite element method. This formulation is quite natural since both equations have an efficient formulation in this form. On the one hand, mixed formulation is used in Galbrun's equation to avoid numerical locking, in the other hand, this is useful in poroelasticity to save degrees of freedom. Under the assumptions there is no flow in the liner and uniform mean flow in the acoustic domain, this method is validated by an analytic method in an infinite duct.

## 1. INTRODUCTION

Porous materials are extensively used in automotive and in aircraft industry for environmental noise reduction. To improve the comprehension and the design, a robust numerical method is needed for this problem. To take these treatments into account, many levels of modeling can be used: local reactive impedance, an equivalent fluid and Biot's model. Only the latter preserves vibro-acoustic interactions, absorption and the propagation in the liner. In recent papers, an efficient mixed formulation in pressure - solid displacement of Biot's equations was proposed by Atalla *et al.* [2]. These authors have already investigated the coupling with elastic structures and acoustical media at rest. Moreover, in aeronautics, the presence of non-potential mean flow complicates the acoustic propagation models. Two equivalent physical models are proposed in the literature: the Linearized Euler's Equations (LEE) and the Galbrun's equation. The latter is written in term of the Lagrangian perturbation of the displacement and allows a direct treatment of the coupling condition at the interface [7], whereas LEE need appropriate condition (Myers [9]). For several years, we have worked on Galbrun's equation and have developed a mixed finite element formulation in pressure - displacement to avoid numerical locking, Treyssède *et al.* [10]. Furthermore, a coupled vibroacoustic model was proposed by Gabard *et al.* [7] and has

shown the great influence of the elastic structure on the acoustics. This work continue with this way of coupling with poroelastic liners.
In the next section, we shall recall some basics of Galbrun's and Biot's equation and propose a coupling formulation. Finally, we validate our numerical model with an analytical solution.

## 2. THEORY

### 2.1. Galbrun's equation

Galbrun's equation derives from general fluid mechanic conservation equations, whereby the linearization process is carried out with a lagrangian perturbation, namely, associated with a fluid particule and not to a geometric point. The direct resolution of harmonic Galbrun's equation with the Finite Element Method (FEM) gives rise to corrupted results with non-structured mesh. To overcome this difficulty, the *mixed FEM formulation* has been introduced and extensively discussed in previous works [7, 10].
Under the assumption of a perfect fluid and an isentropic eulerian flow, the equation can be written in the frequency domain ($e^{-i\omega t}$) as follows :

$$-\rho_0\omega^2\mathbf{w} - 2i\omega\rho_0\mathbf{v_0}\cdot\nabla\mathbf{w} + \rho_0\mathbf{v_0}\cdot\nabla(\mathbf{v_0}\cdot\nabla\mathbf{w}) + \nabla p^L = 0\,, \tag{1}$$

$$p^L + \rho_0 c_0^2\nabla\cdot\mathbf{w} = 0\,. \tag{2}$$

Here, subscripts "0" denotes the mean flow variables, $p^L$ is the lagrangian acoustic pressure and $\mathbf{w}$ the lagrangian displacement perturbation. The associated weak formulation is

$$\begin{aligned}
&-\int_{\Omega_a}\frac{1}{\rho_0 c_0^2}p^{L*}p^L d\Omega + \int_{\Omega_a}\nabla p^{L*}\cdot\mathbf{w}d\Omega + \int_{\Omega_a}\mathbf{w}^*\cdot\nabla p^L d\Omega - \omega^2\int_{\Omega_a}\rho_0\mathbf{w}^*\cdot\mathbf{w}d\Omega \\
&-i\omega\int_{\Omega_a}\rho_0\mathbf{w}^*\cdot(\mathbf{v}_0\cdot\nabla\mathbf{w})d\Omega + i\omega\int_{\Omega_a}\rho_0(\mathbf{v}_0\cdot\nabla\mathbf{w}^*)\cdot\mathbf{w}d\Omega - \int_{\Omega_a}\rho_0(\mathbf{v}_0\cdot\nabla\mathbf{w}^*)\cdot(\mathbf{v}_0\cdot\nabla\mathbf{w})d\Omega \\
&+\underbrace{\int_{\partial\Omega_a}\mathbf{w}^*\cdot\left\{\rho_0(\mathbf{v}_0\cdot\mathbf{n}_a)\frac{d\mathbf{w}}{dt}\right\}dS}_{I_1} - \int_{\partial\Omega_a}p^{L*}(\mathbf{w}\cdot\mathbf{n}_a)dS = 0\,, \quad \forall\left\{\mathbf{w}^*, p^{L*}\right\},
\end{aligned} \tag{3}$$

with the test functions $p^{L*}$, $\mathbf{w}^*$ and $\mathbf{n}_a$ denotes the normal unit vector pointing away from the fluid domain $\Omega_a$. The extension in the three dimensional case has been carried out by Bériot *et al.* [3] and his tetrahedral element T5-4c, will be used in the remainder of the paper. Interpolation is linear for the pressure and a bubble function is added for the displacement in order to respect the inf-sup condition.

### 2.2. Biot's model

#### *2.2.1. Displacement - Displacement original formulation and Biot waves*

For statistically isotropic materials, Biot's model [4] is grounded on the superposition of a fluid phase and a solid phase which are inertially coupled with the effective density coefficient $\rho_{ij}$. Furthermore, the stress tensor, is also a superposition of a solid and a fluid tensor. The original set of equations, gives (4-5) and will be useful in the validation in Section 3. For the numerical implementation, the equivalent Atalla's mixed formulation [2] will be used to simplify coupling

Table 1. Materials properties used in numerical tests

| Mat | $\phi$ | $\sigma$ [kNm$^{-}$4s] | $\alpha_{\text{inf}}$ | $\Lambda$ [$\mu$m] | $\Lambda'$ [$\mu$m] | $\rho_1$ [kgm$^{-}$3] | $E$ [kPa] | $\nu$ |
|---|---|---|---|---|---|---|---|---|
| XFM | 0.98 | 13.5 | 1.7 | 80 | 160 | 30 | 540(1 - $j$0.05) | 0.35 |

conditions and to save computation time. Indeed, only 4 degrees of freedom (dof) per node are needed instead of 6 dof in the $(\mathbf{u}, \mathbf{U})$ formulation.

$$\tilde{P}\nabla(\nabla\cdot\mathbf{u}) - \tilde{N}\nabla\wedge(\nabla\wedge\mathbf{u}) + \tilde{Q}\nabla(\nabla\cdot\mathbf{U}) + \omega^2(\tilde{\rho}_{11}\mathbf{u} + \tilde{\rho}_{12}\mathbf{U}) = 0 \tag{4}$$

$$\tilde{Q}\nabla(\nabla\cdot\mathbf{u}) + \tilde{R}\nabla(\nabla\cdot\mathbf{U}) + \omega^2(\tilde{\rho}_{12}\mathbf{u} + \tilde{\rho}_{22}\mathbf{U}) = 0 \tag{5}$$

$\tilde{A}, \tilde{N}, \tilde{P}, \tilde{Q}, \tilde{R}$ are Biot's coefficients as defined in [1, 4]. $\tilde{A}$ and $\tilde{N}$ correspond to the Lamé coefficients and $\tilde{P} = 2\tilde{A} + \tilde{N}$. $\tilde{R}$ is the bulk modulus of the fluid phase and $\tilde{Q}$ indicates the coupling of the two phases volumic dilatation. We can note that the imaginary part ( "˜" denotes complex coefficients) of $\tilde{A}$ and $\tilde{N}$ includes the structural damping and, in $\tilde{Q}$ and $\tilde{R}$ this part includes the thermal dissipation. Those parameters are function of the material properties given in Table 1 (Here we considered the porous material XFM, see Table 1 in [6]).

*2.2.2. The mixed displacement pressure formulation*

The Atalla's mixed formulation as presented in [2] is

$$\begin{aligned} \nabla\cdot\underline{\underline{\tilde{\sigma}}}^s(\mathbf{u}) + \omega^2\tilde{\rho}\,\mathbf{u} + \tilde{\gamma}\,\nabla p &= 0\,, \\ \Delta p + \omega^2\frac{\tilde{\rho}_{22}}{\tilde{R}}p - \omega^2\frac{\tilde{\rho}_{22}}{\tilde{\phi}^2}\tilde{\gamma}\,\nabla\cdot\mathbf{u} &= 0\,. \end{aligned} \tag{6}$$

Here, $p$ is the pressure in the fluid phase and $\mathbf{u}$ is the solid phase displacement vector, $\tilde{\gamma} = \phi\left(\frac{\tilde{\rho}_{12}}{\tilde{\rho}_{22}} - \frac{\tilde{Q}}{\tilde{R}}\right)$ and $\tilde{\rho} = \tilde{\rho}_{11} - \frac{\tilde{\rho}_{12}^2}{\tilde{\rho}_{22}}$.
The associated weak formulation, considering the test function $p^*$ and $\mathbf{u}^*$, is

$$\begin{aligned} &\int_{\Omega_p}\underline{\underline{\tilde{\sigma}}}^s(\mathbf{u}):\underline{\underline{\varepsilon}}(\mathbf{u}^*)d\Omega - \tilde{\rho}\,\omega^2\int_{\Omega_p}\mathbf{u}\cdot\mathbf{u}^*d\Omega + \int_{\Omega_p}\left[\frac{\phi^2}{\omega^2\tilde{\rho}_{22}}\nabla p\cdot\nabla p^* - \frac{\phi^2}{\tilde{R}}p\,p^*\right]d\Omega \\ &-\int_{\Omega_p}\left[\tilde{\gamma} + \phi\left(1 + \frac{\tilde{Q}}{\tilde{R}}\right)\right](\nabla p^*\cdot\mathbf{u} + \nabla p\cdot\mathbf{u}^*)d\Omega - \phi\left(1 + \frac{\tilde{Q}}{\tilde{R}}\right)\int_{\Omega_p}(p^*\nabla\cdot\mathbf{u} + p\nabla\cdot\mathbf{u}^*)\,d\Omega \\ &-\int_{\partial\Omega_p}\left[\underline{\underline{\sigma}}^t\,\mathbf{n}\right]\cdot\mathbf{u}^*dS - \int_{\partial\Omega_p}\phi\left(U_n^f - u_n\right)p^*dS = 0\,, \quad \forall\{p^*, \mathbf{u}^*\}\,, \end{aligned} \tag{7}$$

where, $\mathbf{n}$ denotes the outward normal unit vector to the poroelastic domain $\Omega_p$.

## 2.3. Coupling method

*2.3.1. Coupling Conditions*

Coupling conditions without flow are summarized by Debergue *et al.* [6] for several configurations. Here, we shall focus on a "direct" coupling, without an impermeable membrane for example, but there is no hindrance to implement them and only (10) is modified.
The first condition, given by (8), comes from the standard continuity requirement of the nor-

mal stress at the interface and remains valid with flow. The second condition (9), ensures the continuity of the pressure and (10), the continuity of the mass flux at the interface. The last two conditions must be satisfied for a fluid particle, *i.e.* in the sense of the lagrangian perturbation. We can note that in the mixed formulation, **w** is a nodal variable and this avoids the need for computing the normal derivative of the acoustic pressure as it is the case for the Helmholtz equation.

$$\left[\underline{\underline{\tilde{\sigma}}}^t\,\mathbf{n}\right] = -p^L \cdot \mathbf{n}\,, \tag{8}$$

$$p = p^L\,, \tag{9}$$

$$w_n = \phi(U_n - u_n) + u_n\,. \tag{10}$$

*2.3.2. Global Formulation*

The global formulation is obtained by summing (3) and (7). Because of the length of expressions, we shall detail only boundary terms on the coupling surface $\Gamma$ in (12). Firstly, the $I_1$ integral in (3) vanishes on $\Gamma$: because there is no flow in the liner, vectors $\mathbf{v}_0$ and $\mathbf{n}_a$ are orthogonal. Both conditions (8) and (10) are directly substituted in boundary terms. But, as for the Biot-Helmholtz coupling, the second condition (9) can not be imposed in the weak formulation. Authors have resorted to Lagrange multipliers or imposed directly the relation in the system. Here, we introduce an additional functional as suggest by Hamdi [2]

$$\int_\Gamma w_n^* \left(p^L - p\right) d\Gamma = 0, \quad \forall \left\{\mathbf{w}^*\right\}\,, \tag{11}$$

and $\mathbf{w}^*$ plays the same role as a Lagrange multiplier. As this condition is added directly in the formulation we could relax the constraint in (9) and replace $p^L$ by $p$. These two manipulations yield a symmetric formulation of the coupling integrals and we get on $\Gamma$

$$\int_\Gamma p \cdot u_n^* d\Gamma + \int_\Gamma p^* \cdot u_n d\Gamma + \int_\Gamma p^L \cdot w_n^* d\Gamma + \int_\Gamma p^{L*} \cdot w_n d\Gamma \\ - \int_\Gamma p^* \cdot w_n d\Gamma - \int_\Gamma w_n^* \cdot p^L d\Gamma = 0, \quad \forall \left\{p^*, \mathbf{u}^*, p^{L*}, \mathbf{w}^*\right\}. \tag{12}$$

The first line of (12) shows the Pressure-displacement coupling in each domain whereas the second gives Pressure-displacement coupling between the two domains. It's worth observing that this coupling is due to a symmetric operator between lagrangian displacement **w** and the fluid pressure in the porous, $p$.

## 3. RESULTS AND VALIDATION

### 3.1. Analytical solution in the case of an uniform mean flow

In order to validate our numerical model, an analytical model with uniform mean flow of Mach number $M$, is established in an infinite duct. In this case, complex mode shape and the axial wave number could be found. To validate our FEM model, we shall evaluate his capacity to propagate these modes.
Guided waves in porous material have been recently used by Boeckx *et al.* [5], in a material

properties identification method context. We propose here an extension to cylindrical coordinate.

*3.1.1. Helmholtz decomposition in cylindrical coordinate*

In the porous material, we could use the Helmholtz decomposition for the fluid and solid displacement to decouple Biot's equation [1]. These fields can be written

$$\mathbf{u} = \nabla\varphi + \nabla \wedge \psi \ , \quad \mathbf{U} = \nabla\chi + \nabla \wedge \Theta. \tag{13}$$

We can note that this decomposition is not unique and an arbitrary condition must be added on vector potentials. After decoupling, we have

$$\varphi = \varphi_1 + \varphi_2 \ , \quad \chi = \mu_1\varphi_1 + \mu_2\varphi_2, \tag{14}$$

where,

$$\mu_i = \frac{\tilde{P}k_i^2 - \omega^2\tilde{\rho}_{11}}{\omega^2\tilde{\rho}_{12} - Qk_i^2}, \quad i = 1, 2 \ , \tag{15}$$

are the waves amplitude ratios between the two phases in the porous material.
Similarly, the vector potential $\Theta$ could be rewritten as

$$\Theta = \mu_3\psi \ , \quad \text{with } \ \mu_3 = \tilde{\rho}_{12}/\tilde{\rho}_{22}. \tag{16}$$

Under this form, each potential fulfills the wave equation with the complex wave numbers given by Eq. (17-19). At least, there are two compressional waves and one rotational wave which can propagate in an isotropic porous material. Each wave is present in the two phases (his importance is given by $\mu_i$) but compressional and rotational wave are not coupled. This is a common result in solid mechanics, but the presence of two phases in the porous material adds a new compressional wave due to the fluid phase and associated to the scalar potential $\phi_2$.

$$k_1^2 = \frac{\omega^2}{2(\tilde{P}\tilde{R} - \tilde{Q}^2)}(\tilde{P}\tilde{\rho}_{22} + \tilde{R}\tilde{\rho}_{11} - 2\tilde{Q}\tilde{\rho}_{12} + \sqrt{\Delta}), \tag{17}$$

$$k_2^2 = \frac{\omega^2}{2(\tilde{P}\tilde{R} - \tilde{Q}^2)}(\tilde{P}\tilde{\rho}_{22} + \tilde{R}\tilde{\rho}_{11} - 2\tilde{Q}\tilde{\rho}_{12} - \sqrt{\Delta}), \tag{18}$$

$$k_3^2 = \frac{\omega^2}{\tilde{N}}\left(\frac{\tilde{\rho}_{11}\tilde{\rho}_{22} - \tilde{\rho}_{12}^2}{\tilde{\rho}_{22}}\right), \tag{19}$$

with $\Delta = (\tilde{P}\tilde{\rho}_{22} + \tilde{R}\tilde{\rho}_{11} - 2\tilde{Q}\tilde{\rho}_{12})^2 - 4(\tilde{P}\tilde{R} - \tilde{Q}^2)(\tilde{\rho}_{11}\tilde{\rho}_{22} - \tilde{\rho}_{12}^2)$.
The pressure $p$ in the fluid phase, given by Biot [4], is deduced from the fluid stress tensor $\underline{\underline{\sigma}}^f$ and porosity $\phi$

$$\underline{\underline{\sigma}}^f = -\phi p \, \underline{\underline{I}} \quad \text{and} \quad -\phi p = \tilde{Q}\,\nabla\cdot\mathbf{u} + \tilde{R}\,\nabla\cdot\mathbf{U} \ . \tag{20}$$

In cylindrical coordinate $(r, \theta, z)$, Gazis [8] gives the general form of the potential expressed in term of Bessel function for hollow elastic cylinders. The extension to the poroelastic requires one additional scalar potential $\phi_2$. Moreover, without loss of generality, the azimuthal mode number is fixed to zero. In the same way the velocity scalar potential could be defined in the acoustic domain under a uniform mean flow assumption, with,

$$k_{ar}^2 = (k_a - Mk_z)^2 - k_z^2, \text{ and } k_a = \omega / c_o \tag{21}$$

### *3.1.2. Dispersion equation*

The coupling conditions are the same as those given Section 2.3.1. We could just mention that the pressure is given with material derivative of the acoustic velocity potential $\phi_a$. In addition we chose a configuration, described in Fig. 1 where the liner is clamped on a the rigid and impermeable wall of the duct. This yields

$$\mathbf{u} = \mathbf{0} \quad \text{and} \quad U_n - u_n = 0 \quad \text{on } \Gamma_r \; . \tag{22}$$

These conditions signify that the solid phase displacement is null as well as the relative normal displacement between the two phases.
The application of coupling conditions and boundary conditions leads to the linear system

$$\mathcal{M}(k_z)\mathbf{A} = \mathbf{0} \; , \tag{23}$$

where $\mathcal{M}(k_z)$ is a 7×7 matrix with analytic components and **A** is the row vector containing the wave amplitudes. The $i^{th}$ complex mode $(k_z^i, \mathbf{A}^i)$ we are looking for corresponds to the non-trivial solution of this system. The numerical solution of the dispersion equation det $\mathcal{M}(k_z) = 0$ is quite difficult and is carried out in two steps. Firstly, a coarse sweep in the complex plan is achieved to locate the $k_z^i$. Then, these values are chosen to initialize an optimization algorithm.

## 3.2. Validation with an uniform mean flow

In this section we shall compare our model with the analytical model. For each case, the analytical solution is imposed on the $\Gamma_{in}$ and $\Gamma_{out}$ surface (depicted in Fig. 1) in the FEM model. In the acoustic domain $\Omega_a$, only the displacement is imposed, whereas in the poroelastic domain $\Omega_p$, both quantities are imposed. In practical configuration this is not an important limitation because the liner is completely confined in the duct. Four elements are used in the radial direction in acoustic domain, 6 in the porous domain and 18 per wave length in the axial direction as shown in Fig. 2-3. It's worth observing that the same mesh have been used to plot the analytic solution. Both fluid domain and porous solid phase displacement fields are plotted on the same figure, that is why fields are discontinuous as indicated by (10) and also why the order of magnitude are quite different, but the pressure continuity is provided.
In Fig. 2-3, we note an excellent agreement between the numerical and the analytical model. Indeed the $\mathcal{E}^2$ error in a section $S$, defined in (24) and summarised in the Table 2, never exceeds 2.6% for all quantities.

$$\mathcal{E}^2(\Phi) = 100 \times \frac{\left\| \Phi^{FEM} - \Phi^{ANA} \right\|_{L_2(S)}}{\left\| \Phi^{ANA} \right\|_{L_2(S)}} \tag{24}$$

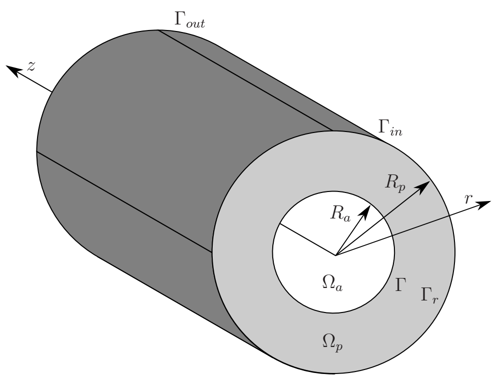


Figure 1. Sketch of the validation problem

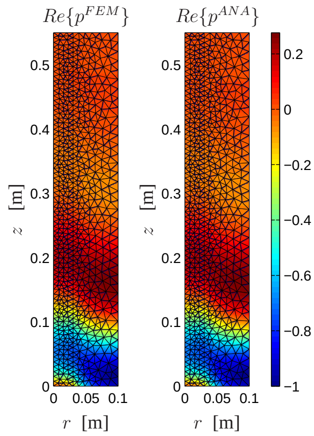


Figure 2. Pressure for $M = 0$, $f = 600$ Hz, $k_z \approx 21.8 + 8.9j$. Air from $r = 0$ to $r = 0.03$ m. XFM from $r = 0.03$ to $r = 0.1$m

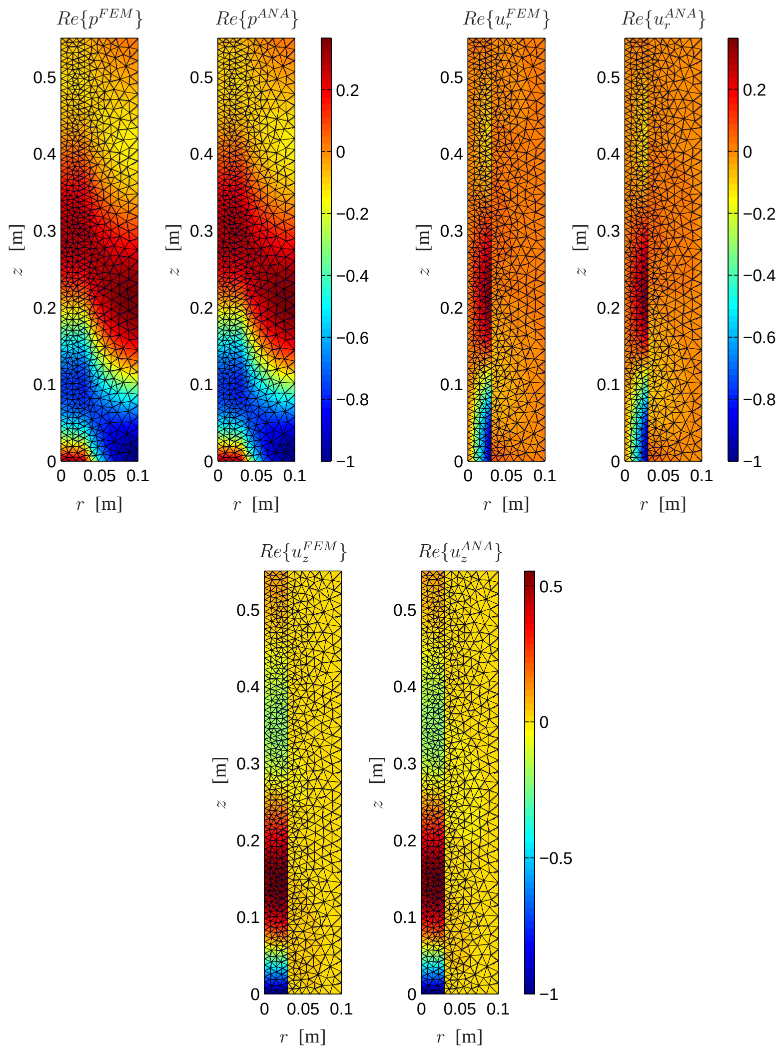


Figure 3. Numerical results (FEM) and analytic results (ANA) for the real part of acoustic quantities for $M = 0.3$, $f = 600$ Hz, $k_z \approx 15.6 + 5j$. Air from $r = 0$ to $r = 0.03$ m. XFM from $r = 0.03$ to $r = 0.1$m

Table 2. Error $\mathcal{E}^2$ for $M = 0.3$, 600 Hz, $k_z \approx 15.6 + 5j$

| Quantity | Pressure | Radial Disp. | Axial Disp. |
|---|---|---|---|
| Error (%) | 1.69 | 1.43 | 2.57 |

## 4. CONCLUDING REMARKS

In the present work, Atalla's mixed FEM formulation of Biot's equation (assuming there is no flow in the liner), was coupled with our mixed FEM formulation of Galbrun's equation. By taking advantage of the two formulations in pressure-displacement, all coupling conditions can be applied naturally. Finally, our coupling terms are symmetric and quite similar to those obtained with a classic Helmholtz's coupling. Our numerical results show a very good agreement with the analytic model and this is engaging to continue to a more applied noise reduction benchmark.

## REFERENCES

[1] J.-F. Allard. *Propagation of Sound in Porous Media: Modeling Sound Absorbing Materials*. 1993.

[2] N. Atalla, M. A. Hamdi, and R. Panneton. Enhanced weak integral formulation for the mixed $(u, p)$ poroelastic equations. *J. Acoust. Soc. Am.*, 109(6):3065 – 3068, 2001.

[3] H. Beriot and M. Ben Tahar. A three dimensional finite element model for sound propagation in non potential mean flows. In *Proceedings of ICSV13*, Vienna, Austria, July 2-6, 2006.

[4] M. A. Biot. Theory of propagation of elastic waves in a fluid-saturated porous solid. I. low-frequency range. *J. Acoust. Soc. Am.*, 28(2):168–178, 1956.

[5] L. Boeckx, P. Leclaire, P. Khurana, C. Glorieux, W. Lauriks, and J. F. Allard. Investigation of the phase velocities of guided acoustic waves in soft porous layers. *J. Acoust. Soc. Am.*, 117(2):545–554, 2005.

[6] P. Debergue, R. Panneton, and N. Atalla. Boundary conditions for the weak formulation of the mixed $(u, p)$ poroelasticity problem. *J. Acoust. Soc. Am.*, 106(5):2393–2390, 1999.

[7] G. Gabard, F. Treyssède, and M. Ben Tahar. A numerical method for vibro-acoustic problems with sheared mean flows. *J. Sound Vib.*, 272:991–1011, 2004.

[8] D. C. Gazis. Three-dimensional investigation of the propagation of waves in hollow circular cylinders. I. analytical foundation. *J. Acoust. Soc. Am.*, 31(5):568–573, 1959.

[9] M. K. Myers. On the acoustic boundary condition in the presence of flow. *J. Sound Vib.*, 71(3):429–434, 1980.

[10] F. Treyssède, G. Gabard, and M. Ben Tahar. A mixed finite element method for acoustic wave propagation in moving fluids based on an eulerian lagrangian description. *J. Acoust. Soc. Am.*, 113(2):705–716, 2003.